Concurrent Implementation of 81 Frequency Elements Together With Frequency Tracking in Protective Relays: Issues and Solutions

Gabriel Benmouyal and Angelo D'Aversa
Schweitzer Engineering Laboratories, Inc.

Presented at the
36th Annual Western Protective Relay Conference
Spokane, Washington
October 20–22, 2009

Concurrent Implementation of 81 Frequency Elements Together With Frequency Tracking in Protective Relays: Issues and Solutions

Gabriel Benmouyal, Angelo D'Aversa, *Schweitzer Engineering Laboratories, Inc.*

***Abstract*—The use of 81 elements (over or under-frequency functions) necessitates the proper measurement of the local frequency. In many modern relays, the frequency measurement is based upon the voltage or current waveforms, the sampling of which is under the control of the technique known as adaptive sampling or frequency tracking. In this situation, the frequency measurement and the frequency tracking are tied together, resulting in undesirable frequency measurement transients. The purpose of this paper is to introduce techniques that will render frequency measurement and frequency tracking completely independent from each other, allow the frequency measurement to be free of any transient resulting from the adaptive sampling, and to exhibit an acceptable dynamic response.**

I. Introduction

In many digital protective relays or intelligent electronic devices (IEDs), an independent circuit separate from the microprocessor accomplishes frequency measurement for the purpose of implementing 81 elements (81O over or 81U under-frequency elements) Implementation of the protective functions and elements occurs within the microprocessor. One disadvantage of this solution is that we need additional hardware components to measure the frequency, and this degrades the overall reliability of the relay.

With the advent of more powerful microprocessors and the proliferation of numerical algorithms to measure the signal (voltages and currents) frequency, it has become common to compute the local frequency in the same microprocessor or controller that implements the protective functions.

Two sampling techniques are available to acquire the voltage and current instantaneous samples: fixed sampling frequency and adaptive sampling frequency. Existing literature describes scores of algorithms to measure the frequency using a fixed sampling frequency, and some of these algorithms have been applied in relays. This paper addresses only the seldom documented issue of calculating the frequency by using adaptive sampling. Assuming that we acquire the instantaneous samples of the signal at a rate of N samples-per-cycle of the signal's frequency SIGFREQ, with an adaptive scheme, the sampling frequency SAMFREQ will vary depending upon the local network frequency and can be calculated in steady state as follows:

$$\text{SAMFREQ} = N \bullet \text{SIGFREQ} \tag{1}$$

Based on this simple equation, one might be tempted to infer that a straightforward frequency measuring algorithm could be devised by simply dividing the sampling frequency by the number N as in the following equation:

$$\text{SIGFREQ} = \frac{\text{SAMFREQ}}{N} \tag{2}$$

This paper will demonstrate that although this conclusion is applicable in steady state, things become more complicated in transient state where the basic principle of (2) is no longer applicable. When the purpose of the frequency measurement is to implement 81 elements, special precautions are necessary to get a frequency measurement that will have an acceptable dynamic response in transient state. In this paper, we explain that the frequency measurement must comply with some basic dynamic requirements to yield acceptable frequency functions.

II. Frequency Tracking in Digital Relays

A. Principles of Digital Filtering of Waveforms in Numerical Relays

A numerical protective relay, after it acquires voltage and current waveforms at some sampling frequency, processes these waveforms instantaneous samples through a digital filter for the purpose of extracting the waveform fundamental frequency phasor. Among the most popular digital filtering systems are the half- or full-cycle DFT filter or its offshoot, the half- or full-cycle Cosine filter [3]. The full-cycle DFT filter uses a data window of N samples according to the following equation to compute a waveform fundamental phasor:

$$X = \frac{2}{N}\sum_{k=0}^{N-1} x(k\Delta T) \bullet e^{-j\frac{2\pi k}{N}} \tag{3}$$

A full-cycle Cosine filter calculates a waveform fundamental phasor following (4):

$$X = \frac{2}{N}\sum_{k=0}^{N-1}\left(x(k\,\Delta T) - j\,x\left[(k+\frac{N}{4})\Delta T\right]\right) \bullet \cos\frac{2\pi k}{N} \tag{4}$$

A particularity of these numerical filtering systems is that they have a magnitude and phase frequency response and that they will calculate the fundamental phasor properly only when the sampling frequency is a multiple of the signal frequency, the multiple being the number N equal to the number of samples in one cycle of the signal frequency.

When applying (3) or (4), one gets a signal phasor that rotates counterclockwise in the complex plane with steps of

360/N degrees. The phasor can be made still or time-invariant in the complex plane by multiplying the rotating phasor by a unit phasor that rotates in the reverse direction (clockwise) with the same angular step [9].

We select a Cosine filter in relays because this filter exhibits a better rejection than the Fourier filter for any exponentially decaying component present in current signals during a fault. We can use a Cosine filter without a high-pass filter to reject a dc component, and the Cosine filter will be more immune to high-frequency noise than a Fourier filter ([3] [10]).

Fig. 1 represents the normalized magnitude frequency response of a full-cycle Cosine filter. The filter exhibits a unity gain at the frequency corresponding to the sampling frequency divided by the number of instantaneous samples N in one cycle. As an example, if the sampling frequency is 960 Hz and N = 16, unity gain occurs at 60 Hz.

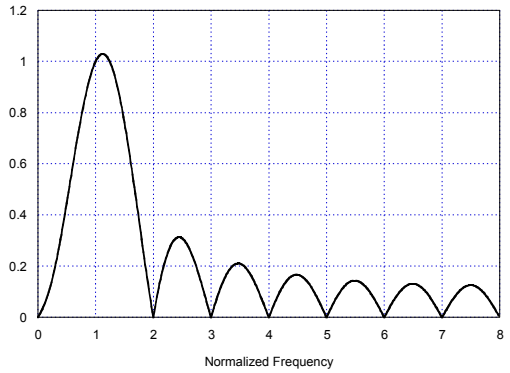

Fig. 1. Normalized magnitude frequency response of the Cosine filter

For a particular signal, a filter data window is the number of instantaneous samples the filter must process to acquire a waveform phasor. We assume here that the waveform has constant magnitude, phase angle, and frequency. Assuming a sampling frequency of N = 16 samples per cycle, a full-cycle Fourier filter has a data window of 16 samples. A half-cycle Fourier filter data window has 8 samples. A half-cycle Cosine filter will have a data window of 12 samples, whereas the full-cycle version of the same filter has a data window of 20 samples.

When we acquire a phasor by means of a Fourier or Cosine filter, there are two well-known situations where the phasor calculation creates a transient: a change in the waveform magnitude or a change in the phase angle.

Transmission line voltage waveforms undergo a reduction in magnitude at the occurrence of a fault. During this time, we will assume that the frequency remains constant. Let us further assume that we use a Cosine filter with a sampling rate of 16 samples per cycle. We need to have 20 samples in the waveform data window corresponding to the fault condition before the waveform phasor will be error-free and its magnitude and phase angle will equal the steady state of the fault condition. During the interval of time when some of the older samples in the data window correspond to the pre-fault condition, the calculated waveform will be in transient state (i.e., it will exhibit an error in magnitude and phase angle with respect to the final values corresponding to the fault conditions).

The interval of time necessary to change all the samples in a waveform data window so that they correspond to a new condition is commonly called the filter nominal response time. A full-cycle Fourier filter has a response time of one cycle and a full-cycle Cosine filter has a response time of one and a quarter cycles.

B. Principles of Frequency Tracking Implementation in Digital Relays

To allow a relay to compute voltage and current phasors on a broad enough frequency interval, protective and signal processing engineers have devised a technique commonly known as frequency tracking. Fig. 2 shows the basic implementation of the frequency tracking principle. It consists of the following:

1. We calculate the necessary sampling frequency SAMFREQ by multiplying N times the measured signals frequency SIGFREQ.
2. The IED or the relay controller calculates a preset count by dividing the system clock frequency C by the desired sampling frequency as follows:

$$\text{Preset Count P} = \frac{\text{System Clock C}}{\text{SAMFREQ}} \tag{5}$$

The main component of the frequency tracking circuit is therefore a programmable interval generator. The interval generator is supplied with a clock at frequency C Hz.

3. After the interval generator has been supplied with the proper preset count P, it will generate pulses at the frequency corresponding to the sampling frequency.
4. We supply the sampling pulses to the sample-and-hold line of the circuit acquiring the analog waveforms.

Fig. 2 shows the acquisition of three voltage waveforms for the three phases, but the principle could be extended to any number of channels.

As the preset count P changes to track the signal frequency, at the output of each sample-and-hold device, a waveform sampled at a frequency corresponding to N times the signal frequency SIGFREQ will be available for further processing through the multiplexer and analog-to-digital converter.

C. Phasor Transient State During a Change in Frequency

We have already examined the situation where a change in the magnitude or the phase angle of a waveform creates a transient in the calculation of the corresponding phasor. A less known phenomenon that causes a transient in the phasor calculation is a change in the sampling frequency.

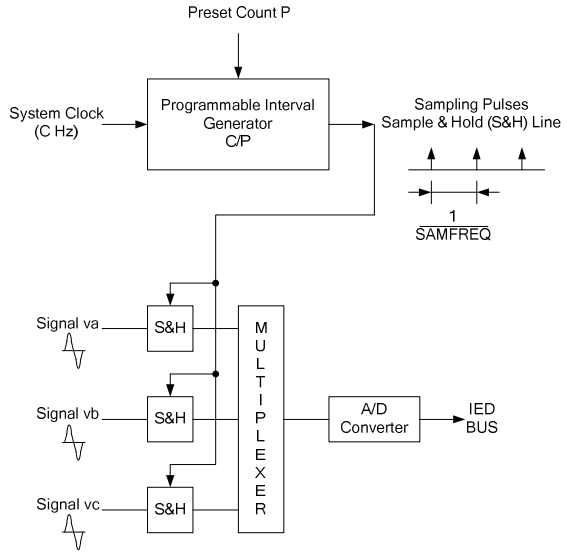

Fig. 2. Principle of frequency tracking circuitry

Let us assume that we use the principle of frequency tracking to acquire the instantaneous samples of a waveform and that the waveform changes frequency before it settles to some final frequency. During the time the change is taking place, the filters will not acquire the waveform instantaneous samples in the corresponding data window with the sampling frequency corresponding to the final frequency value. Therefore, during that same time-interval, the calculated phasor will be in transient state (i.e., it will exhibit an error in magnitude and phase angle with respect to its steady-state value).

D. The Justification for Frequency Tracking in Digital Relays

It is beyond the scope of this paper to review for each protective function all the problems encountered when a digital relay does not compensate for the phasors calculation of frequency excursions. Following some of the major blackouts that have occurred in North America in the recent past (the North-East US-Canadian blackout during August 2003 in particular), we have witnessed a surge of interest in this topic when protection engineers realized that many relays misoperated during large frequency excursions with high rate-of-change of frequency. The topic of how modern digital relays behave has been consequently the object of some excellent reports ([5] [6] [7]). We will illustrate here two situations where frequency tracking is an absolute necessity: elements based on magnitude estimation and elements using a memory.

Phasor magnitude estimation undergoes substantial distortion when the sampling frequency does not correspond to the signal frequency. Fig. 3 illustrates the magnitude acquisition by a Cosine filter of a unit sine-step at 70 Hz using a sampling frequency of 960 Hz (or 16 samples per cycle at 60 Hz). The sampling frequency difference with respect to rated signal frequency is therefore $\Delta f = 10$ Hz. As indicated in [7], the magnitude oscillation will be proportional to $\sin(\pi \Delta f)$, and the oscillation frequency will be twice the signal frequency (or 2 times SIGFREQ in Hz). The magnitude that normally should be flat at level 1 reaches peaks of 1.15 and valleys at 0.9. The consequence of this is that some elements, such as an overvoltage element (59), could overreach. A classical example is a hydroelectric synchronous generator that will accelerate, practically without limit, following a loss of load. An overvoltage element could overreach if the phasor magnitude acquisition is not properly compensated [7].

Fig. 4 illustrates the acquisition of a 50 Hz sine-step by the same Cosine filter at the same sampling frequency of 960 Hz. The phasor magnitude that is also supposed to be flat at level 1 reaches peaks now at 0.97 and valleys at 0.75. An overvoltage (59) element could now underreach when an undervoltage element (27) could overreach.

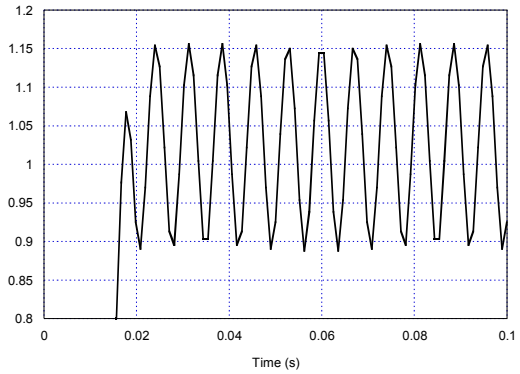

Fig. 3. Cosine-filter magnitude acquisition of a 70 Hz sine-step

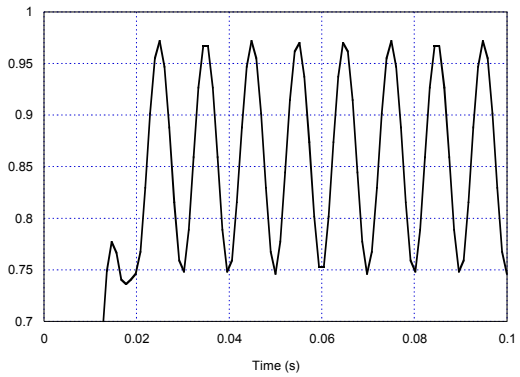

Fig. 4. Cosine-filter magnitude acquisition of a 50 Hz sine-step

Another situation that has drawn the attention of protection engineers recently ([5] [7]) is that of elements that incorporate memory action. As an example, assume implementation of a conventional impedance or distance element (21) with a mho characteristic by defining one operating vector and one polarizing vector as in the following:

$$\begin{aligned} Sop &= m \bullet ZL \bullet Ir - Vr \\ Spol &= Vpol \end{aligned} \tag{6}$$

In this last equation, m is the element reach, ZL is the line positive-sequence impedance, Ir is the current at the input of the element, and Vr is the voltage at the input of the element.

Conventional voltage polarizing quantities Vpol include self-polarization, cross-polarization, polarization by positive sequence phasor (PSP) voltage V1, and, finally, polarization by positive sequence voltage memory (V1M).

The element asserts when the scalar product between the operating quantity and the polarizing quantity is positive or when it satisfies (7):

$$P = \text{real}[m \bullet ZL \bullet (Ir - Vr) \bullet \text{conj}(V_{pol})] \quad (7)$$

In this last equation 'real' represents 'real part of', and 'conj' stands for 'conjugate of'. The scalar product is tantamount to implementing an angle comparator: if the angle between the polarizing quantity and the operating quantity becomes smaller than 90 degrees, the element asserts.

An alternate solution to the scalar product of (7) is to calculate the reach m as follows:

$$m = \frac{\text{real}[Vr \bullet \text{conj}(V_{pol})]}{\text{real}[ZL \bullet Ir \bullet \text{conj}(V_{pol})]} \quad (8)$$

and then to compare the calculated m value to some reach threshold [4]. The advantage of this alternate method is that m is calculated once and for all and is used to establish all the required zones. Another advantage is that, provided the fault resistance is small, m will equal a value close to the distance to the fault.

It is a very well-known phenomenon that when two waveforms with a frequency difference Δf are sampled with the same sampling frequency (where the sampling frequency is a multiple of one of the two waveforms) the angle between the two corresponding phasors will rotate at a speed proportional to the frequency difference Δf. We observe the same phenomenon if the same waveform is sampled at two different sampling frequencies. When there is a memory in the polarizing voltage, this is precisely the phenomenon that takes place. When there is a frequency swing, the vector corresponding to the operating quantity and the vector corresponding to the polarizing quantity are not sampled at the same frequency because there is a proportion of the polarizing waveform that has been acquired earlier when the waveform had a different frequency. The angle between the two vectors (operating and polarizing) will start to shift from the steady-state value. This occurs not because of a change in the power system conditions, but because of the mismatch in the sampling frequencies of the waveforms associated with the two vectors. Ultimately, as a result of the rotation between the two vectors, the angle between the two vectors could become less than 90 degrees and the mho element will misoperate.

If there is no memory effect in the polarizing quantity, all waveforms in the operating and polarizing quantities are digitized using the same sampling frequency, and there is a reduced shift of the angle between the two operating and polarizing vectors. Therefore, self-polarized and cross-polarized mho elements are less affected by frequency swings. Mho elements that include a percentage of memory in the polarizing quantity are affected by network frequency swings and could misoperate under certain conditions.

The worst-case scenario corresponds to the combination of the follow conditions:

- the mho element with the highest reach
- a heavily loaded line (as load increases, the angle between Sop and Spol approaches 90 degrees or could becomes less than 90 degrees with a subsequent misoperation resulting from load)
- a high proportion of memory in the polarizing quantity
- a ramping network frequency with a high value of Hz/s

To illustrate this phenomenon, let us consider among the six possible impedance loops the one covering the A-phase-to-B-phase faults. For the element covering this fault type, Vr is equal to (VA – VB) and Ir is equal to (IA – IB). Let us assume that we use the voltage PSP memory for the polarization, so that we obtain the following:

$$\begin{aligned} Sop &= m \bullet ZL \bullet (IA - IB) - (VA - VB) \\ Spol &= V1M \angle 30° \end{aligned} \quad (9)$$

The voltage PSP memory is calculated according to equations ([4] [7]):

$$V1M(t) = (1 - \alpha) \bullet V1M(t - \Delta t) + \alpha \bullet V1(t) \quad (10)$$

Let us assume now that the three voltages and three currents take the next mathematical form:

$$\begin{aligned} va(t) &= V\sin(2\pi 60t + \theta(t)) \\ vb(t) &= V\sin(2\pi 60t + \theta(t) - 120°) \\ vc(t) &= V\sin(2\pi 60t + \theta(t) + 120°) \end{aligned}$$

$$\begin{aligned} ia(t) &= I\sin(2\pi 60t + \theta(t) - \varphi) \\ ib(t) &= I\sin(2\pi 60t + \theta(t) - 120° - \varphi) \\ ic(t) &= I\sin(2\pi 60t + \theta(t) + 120° - \varphi) \end{aligned} \quad (11)$$

V and I are secondary values. We obtain the secondary load impedance as according to the following:

$$Z_{LOAD} = \frac{V}{I} \angle \varphi \quad (12)$$

For the purpose of the demonstration, let us set the variable as follows (secondary values):

$$\begin{aligned} V &= 69 \text{ Volts} \\ I &= 2 \text{ Amp} \\ \varphi &= 15° \\ \alpha &= 0.2 \\ m \bullet ZL &= 90 \angle 84° \ \Omega \end{aligned} \quad (13)$$

Remember that with these parameters, the combination of the load and the high reach value brings the angle between Vop and Spol to 91.6 degrees; this is close to misoperation. Note also the high percentage of voltage memory (80 percent).

In the first experiment, we set $\theta(t)$ equal to zero, so that the signal frequency will be at exactly 60 Hz. In the second experiment, we set $\theta(t)$ equal to the next expression:

$$\theta(t) = -0.5 \bullet t^2 \quad (14)$$

This time-variable phase angle θ(t) is equivalent to having a changing signal frequency with a rate of change equal to –1 Hz/s:

$$\text{frequency}(t) = 60 - 1 \bullet t \tag{15}$$

Fig. 5 illustrates the impact of the ramping frequency on the angle between the operating and polarizing vectors. With the signals frequencies at 60 Hz, the angle is stable at 91.6°. With the ramping frequency, the angle starts to oscillate and eventually drops below 90 degrees after about 0.6 s, with subsequent misoperation of the element.

Fig. 6 illustrates the same phenomenon by looking at the time trajectory of the scalar product. When the frequency is fixed at 60 Hz, the scalar product is constant and negative, and the mho element will not operate. With no frequency tracking, and when the frequency is ramping at a rate of –1 Hz/s, the scalar product will start to oscillate and will become positive a little after 0.6 s. The mho element will misoperate then.

Fig. 7 shows the variation of the A-phase voltage magnitude as the frequency ramps down to 59 Hz. In another section of this paper, we explain how frequency tracking will correct both situations: element misoperation and magnitude acquisition.

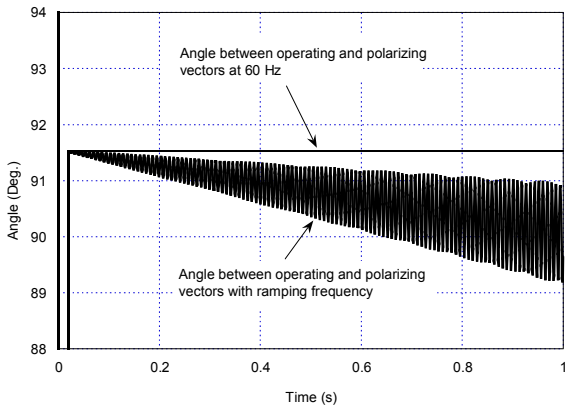

Fig. 5. Angle between operating and polarizing vectors at 60 Hz and ramping frequency without frequency tracking

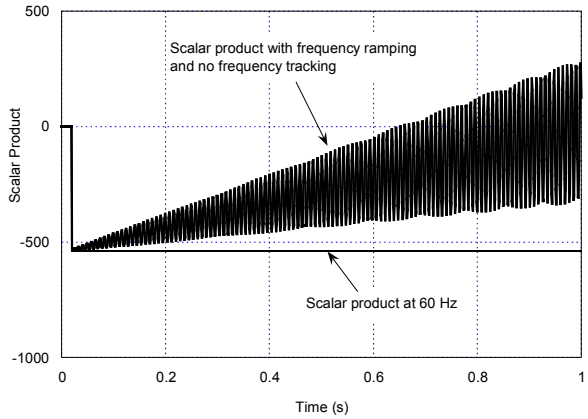

Fig. 6. Mho element scalar product at 60 Hz and with ramping frequency without frequency tracking

Bear in mind here that the same phenomenon would have taken place if, instead of the scalar product, we would have used the distance calculation of (3). Performing the m calculation of (3) is equivalent mathematically to performing the scalar product of (2).

E. The Practice of Frequency Tracking in Relays

If we categorize relays based on frequency tracking, relays can be divided into two classes: transmission line and distribution relays on one side and synchronous generator and motor relays on the other side.

The two classes of relays share an ability to operate with a sampling frequency corresponding to the rated frequency in the absence of input signals

Transmission line and distribution relays will practically operate all the time with the network frequency close or equal to rated frequency. They will, however, undergo frequency excursions as a result of disturbances occurring on the network. For this reason, the interval of frequency tracking will be limited to a few hertz around the rated frequency. Typically, frequency tracking will cover a minimum interval of ±5 hertz around 60 Hz.

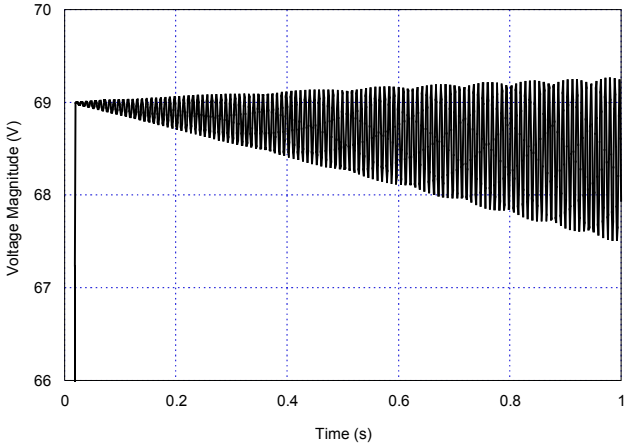

Fig. 7. Magnitude of VA voltage with ramping frequency without frequency tracking

Synchronous generator relays must cope with a start-up and shut-down procedure that can vary from one turbine type to another. Before completing the synchronizing procedure that ties a generator to the network, the different protective functions have to be operational and relays must have acquired the voltage and current phasors properly. Furthermore, and as we already noted, some generators could be the object of substantial acceleration with rapid change of frequency as would happen with a hydroelectric unit following a total or partial loss of load. With rotating machinery, the interval of frequency tracking has to be therefore as broad as possible, typically spanning a minimum range of 20 to 70 Hz.

Finally, whereas with a transmission line relay an increase or decrease of the sampling frequency will always occur around the rated frequency of 60 Hz, a generator relay will be the object of a brutal step-change in the sampling frequency during startup. In this situation, the relay must switch from the sampling frequency at rated frequency (corresponding to the absence of signal) to the low frequency of the minimum signal it can detect upon application of voltage to the field winding.

F. Independent Frequency Tracking and Frequency Measurement in Relays

Many relays incorporate a frequency tracking feature, but they offer a frequency measurement that the relay does not process digitally. In such a situation, frequency tracking and frequency measurement can be considered as completely independent. Fig. 8 presents an example of such an application. It has the following features:

1. The frequency tracking is accomplished following the principles described previously.
2. The three voltages waveforms are supplied to an analog circuit performing a linear combination of the three voltages. The linear combination ensures that if we lose one voltage, we can still use the remaining two phases to calculate the frequency.
3. A low-pass filter follows the linear adder.
4. A comparator and squarer generate a rectangular pulse corresponding to the waveform positive half cycle. The pulse width would be equal to 8.333 ms at 60 Hz. A more advanced version of the application could generate a pulse corresponding to the waveform negative cycle as well. The diagram does not show this.
5. An AND gate controls the arrival of oscillator pulses to a counter. As an example, with an oscillator frequency equal to 7.2 MHz, the counter exhibits a count of 60000 at the end of the pulse with a width of 8.333 ms. This count therefore corresponds to a frequency measurement of 60.000 Hz.

The main advantage of this circuit is that we get a frequency measurement that is completely independent from the frequency tracking and which does not use the sampled values of the voltages for the purpose of computing the frequency.

The drawback of the circuit is that it requires additional components and it does not benefit from the flexibility of a digital implementation.

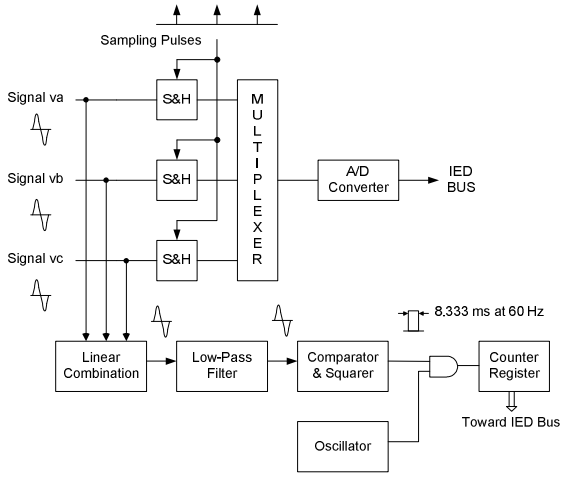

Fig. 8. Example of independent frequency tracking and frequency measurement

III. Principles of Frequency Measurement Concurrently With Frequency Tracking

A. Frequency Measurement Using Adaptive Sampling

Let us assume now that we want to compute the frequency digitally using the instantaneous samples of voltage or current waveforms that have undergone the process of an adaptive sampling rate. Let us assume further that we compute the three-phase voltage phasors (VA, VB, and VC) by means of a full-cycle Cosine filtering system. We obtain the voltage PSP from the following:

$$V1 = (1/3) * (VA + a \bullet VB + a^2 \bullet VC) \tag{16}$$

It has been established that if the sampling frequency corresponds exactly to N times the signal frequency, the voltage PSP will still be in the complex plane. If, however, there is a discrepancy between the sampling rate and the signal frequency, the voltage PSP will rotate in the complex plane at a rate proportional to the frequency deviation [8]. Let us assume that we measure the angular rotation Ψ_m (Fig. 9) of the voltage PSP during an interval of time t_m. The difference in the signal frequency with respect to the sampling frequency can be computed as according to the following:

$$\Delta f = \frac{\Psi_m}{2\pi t_m} \tag{17}$$

We can now calculate the signal frequency SIGFREQ:

$$SIGFREQ = \frac{SAMFREQ}{N} + \Delta f \tag{18}$$

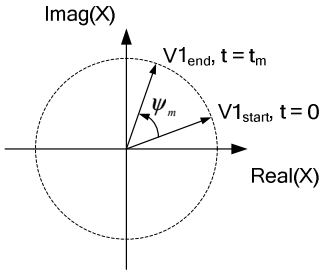

Fig. 9. Rotation of the voltage PSP

Assume that we measure the angular displacement every quarter of a cycle. We can then obtain the frequency deviation from the following:

$$\Delta f = \frac{\Psi_m}{2\pi \dfrac{4}{SAMFREQ}} \tag{19}$$

We can then calculate the angular rotation:

$$\Psi_m = a\tan\left[\frac{imag(V1_{end})}{real(V1_{end})}\right] - a\tan\left[\frac{imag(V1_{start})}{real(V1_{start})}\right] \tag{20}$$

We can then finally calculate:

$$\Delta f = \frac{a\tan\left[\frac{\text{imag}(X_{end})}{\text{real}(X_{end})}\right] - a\tan\left[\frac{\text{imag}(X_{start})}{\text{real}(X_{start})}\right]}{2\pi\frac{4}{\text{SAMFREQ}}} \quad (21)$$

Combination of equations (18) and (19) provides the mathematical means for computing the signal frequency.

B. Concept of a Closed-Loop Feedback System to Establish Sampling Frequency

Equations (17) and (18) have constituted the basis for a feedback closed-loop system to establish the sampling frequency in a relay or an IED. Combining the two equations and expressing Ψ_m as a function of SIGFREQ and SAMFREQ, we obtain the following:

$$\psi_m = 2\pi t_m \bullet \left(\text{SIGFREQ} - \frac{\text{SAMFREQ}}{N}\right) \quad (22)$$

When the angle Ψ_m equals zero, the sampling frequency corresponds to the signal frequency. When there is a discrepancy, the angle assumes some non-zero value. The angle Ψ_m, therefore, constitutes an error signal. This observation leads to the closed-loop feedback system of Fig. 10. At a regular interval, the system uses (20) to calculate the error or angle Ψ_m. The system then calculates the frequency deviation from (21). The system then integrates the frequency deviation to get a new value of the sampling frequency until the sampling frequency corresponds to the signal frequency. When this state is reached the feedback system locks and we will have the equality:

$$\text{SIGFREQ} = \frac{\text{SAMFREQ}}{N} \quad (23)$$

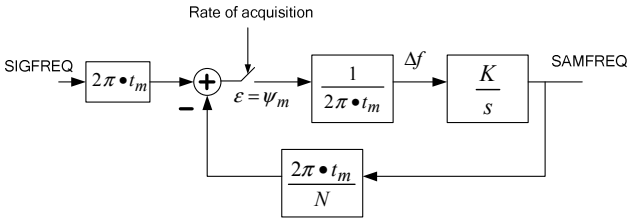

Fig. 10. Conceptual feedback system to establish the sampling frequency

In reality, the model of the feedback system is more complex than the conceptual diagram of Fig. 10. First, we have neglected all the filtering involved in the calculation of the voltage PSP rotation angle Ψ_m. Second, the calculation of the signal frequency will implement some filtering so that we will evaluate an averaged frequency measurement MESFREQ over a number of P samples as in the following:

$$\text{MESFREQ} = \frac{1}{P}\sum_{n=1}^{P}\text{SIGFREQ}_n \quad (24)$$

Third and finally, the new sampling frequency will be calculated using an infinite impulse response filter (IIR) of the type [7]:

$$\text{SAMFREQ}_{new} = M \bullet \text{MESFREQ} + (N - M) \bullet \frac{\text{SAMFREQ}_{old}}{N} \quad (25)$$

In this last equation, M is an integer number, the maximum value of which is (N – 1), which allows us to control the rate of change of the sampling frequency. The purpose of this filtering effect is to prevent an instantaneous change of the sampling frequency following the measurement of a frequency deviation. Obviously, the larger the value of M, the faster the change in the sampling frequency will take place.

C. The Concept of the Time Response to a Frequency Step of a Closed-Loop System

As Fig. 10 shows, frequency tracking constitutes a control closed-loop system where the output variable is the sampling frequency SAMFREQ and the input or regulating variable is the network frequency SIGFREQ. At steady state, the sampling frequency is a multiple of the network frequency:

$$\text{SAMFREQ} = N \bullet \text{SIGFREQ} \quad (26)$$

It is beyond the scope of this paper to revisit the basic principles of control theory as applied to feedback systems. We will concentrate on some essential basic notions that will help us define the best possible control loop. First of all, by looking at the simplified model of Fig. 10, we can infer that the system is basically stable because we only have a single integrator in the open-loop transfer-function. Second, we are interested in the transient response of the frequency measurement when a change occurs in the signal frequency. To evaluate this issue, we will use the concept of deadbeat performance as defined in control theory [1]. In this latest reference, page 118, we have the following definition: "By deadbeat performance is meant that a system responds to a stepwise input in the quickest manner without overshoot."

We have to apply this definition with some caution in the situation of a feedback system for the purpose of frequency tracking and frequency measurement, because we are not necessarily interested in a system with the quickest response. We do not want to be faster than the response time of the phasor filtering system, and we do not want to respond instantaneously to any spurious variation of the frequency that does not correspond to a real variation. We do, however, want to have the minimum possible overshoot.

Some power or protection engineers might argue that a frequency step does not exist on a power system, because frequency is related to the rotation of the synchronous generators and a step-change cannot take place on a generator because of the inertia of the machine. That having been said, the fact remains that the step response is the best tool available to evaluate the dynamic and transient response of the closed-loop system that we are using.

Assume that there are no inputs to the relay or IED and that we apply the three-phase voltage waveforms with a frequency

of 61 Hz. In Fig. 11, we have represented hypothetical frequency time responses to the frequency-step. Let us assume that a desirable response time would be between two and six cycles. Here, the response time is the time it takes for the frequency time trajectory to reach the value of the step-input.

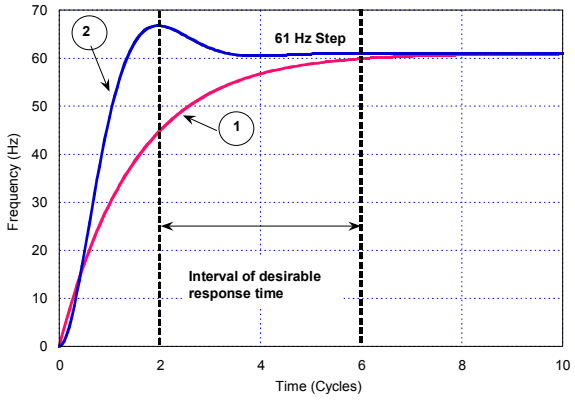

Fig. 11. Examples of response to step-input time trajectories

Looking at the hypothetical response corresponding to trace 1, one can see that we do not have any overshoot, but the response time is a bit marginal and a little longer than six cycles. In classical control theory [2], trace 1 corresponds to what is called an over-damped system. Looking at trace 2, we have a substantial overshoot, but the response time is satisfactory. In classical control theory [2], trace 2 corresponds to what is called an under-damped system. As a preliminary conclusion, neither trace in Fig. 11 represents an acceptable transient response to a step function.

In Fig. 12, we have represented what should be an ideal response to a frequency step-function. We have set the response time to three cycles, which falls inside the interval we want of between two to six cycles. The overshoot is negligible and ideally equal to zero. Finally, the rise to the 61 Hz step-value is steady and linear. The question now is whether we can achieve this ideal response with the phase-locked loop of Fig. 10?

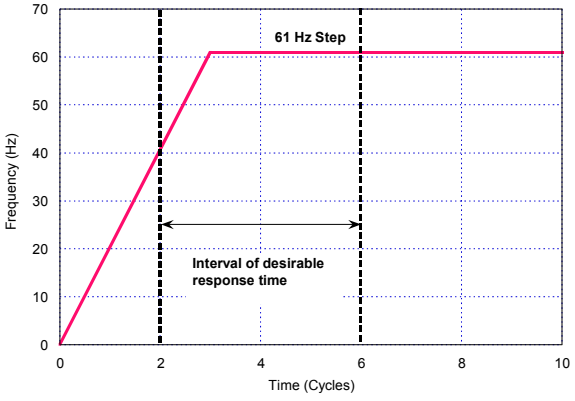

Fig. 12. Ideal response to a 61 Hz step-function

IV. Concurrent Frequency Tracking and Frequency Measurement: Issues

Consider the feedback system of Fig. 10. We have a number of variables to control and adjust the dynamic and transient response of the frequency measurement. These variables are as follows:

1. The rate of acquisition of the angle error. This rate is fixed at one quarter of a cycle. SIGFREQ could vary, so this rate could have different time width.
2. The parameter P that is the number of frequency measurements as provided by (24) from which the system calculates the filtered frequency.
3. The parameter M in (25) that controls the rate of change of the sampling frequency.

Fig. 13 is the flowchart of the routine to calculate the variables SIGFREQ, MESFREQ, and SAMFREQ. The system calls the routine every quarter cycle. At the end of the routine, we proceed with the change of the sampling frequency.

With P = 6 and M = 14, Fig. 14 shows the trajectory of the frequency measurement (MESFREQ) to a step-function of 61.75 Hz. Fig. 15 shows the trajectory of the corresponding sampling frequency (SAMFREQ). Obviously, the response to the step is not satisfactory. We have a huge overshoot, and the response time is greater than 15 cycles.

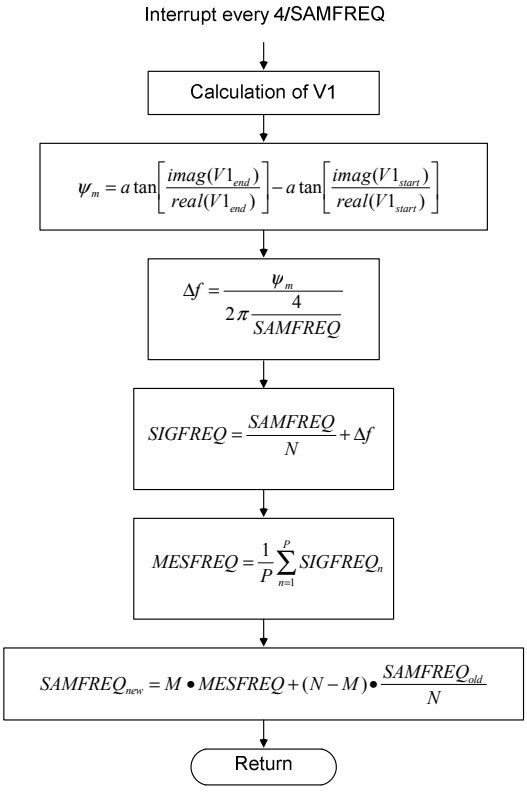

Fig. 13. Calculation of sampling frequency every quarter of a cycle

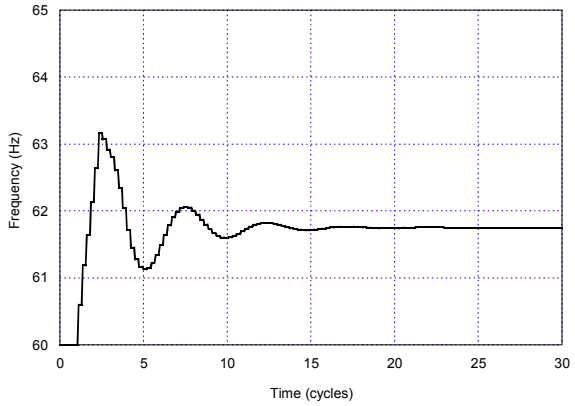

Fig. 14. Time trajectory of MESFREQ with a 61.75 Hz step (P = 6, M = 14)

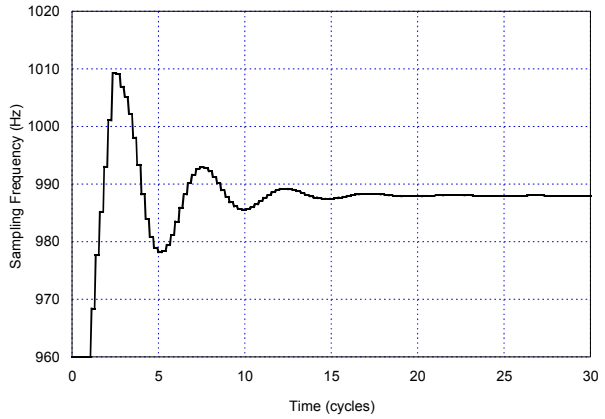

Fig. 15. Time trajectory of SAMFREQ with a 61.75 Hz step (P = 6, M = 14)

To remove the overshoot, we extended the averaging parameter P to 20 and set the M to 6. Fig. 16 shows the corresponding frequency time trajectory, and Fig. 17 shows the sampling frequency time trajectory. We have been able to reduce, but not eliminate, the overshoot, and the time response does not exhibit any improvement with respect to the previous example.

By using the timing scheme corresponding to Fig. 13, and by playing with the various parameters, we have not been able to find time response to a frequency-step close to the ideal of Fig. 12. We discovered a basic shortcoming with this scheme and the next paragraph will describe the nature of the shortcoming along with a resolution.

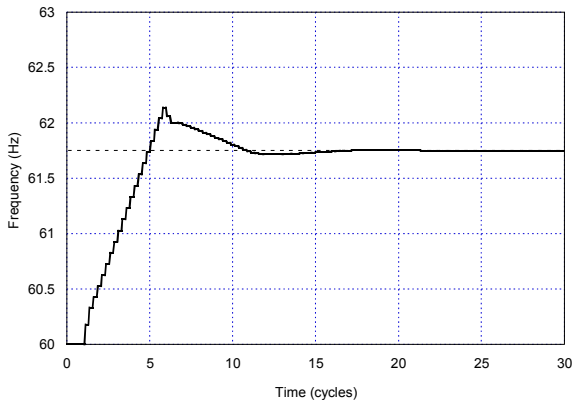

Fig. 16. Time trajectory of MESFREQ with a 61.75 Hz step (P = 20, M = 6)

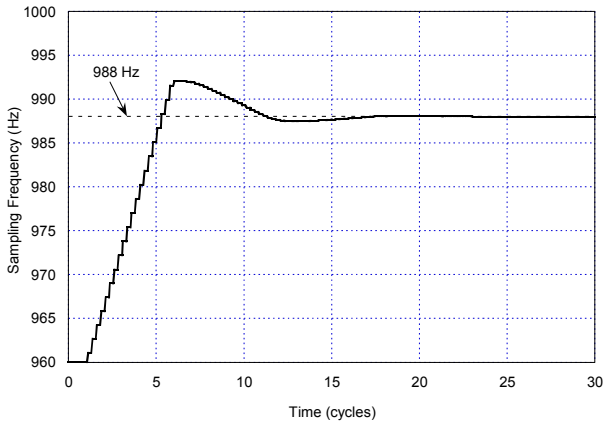

Fig. 17. Time trajectory of SAMFREQ with a 61.75 Hz step (P = 20, M = 6)

V. Concurrent Frequency Tracking and Frequency Measurement: Solutions

There is a basic shortcoming with the timing scheme of Fig. 13. It has its origin with the fact that we are changing the sampling frequency at each quarter cycle following the calculation of a new frequency. The shortcoming is related to the introduction of a transient in the filtering system. As we already noted, when we use frequency tracking, there is a third way to create a transient in the phasor calculation. Such a transient could result from a change in the waveform frequency.

That is exactly what is happening here when we change the sampling frequency following a new measurement of the frequency. As we change the sampling frequency every quarter cycle, we end up with a table of instantaneous values for a waveform where we could have five different sampling frequencies, as Fig. 18 illustrates. When we calculate the phasor based on this table, we introduce a transient state that will impact and introduce an error in the voltage PSP angle Ψ_m. This error in the angle will introduce an error in the calculation of Δf and, consequently, in the calculation of SIGFREQ, MESFREQ, and SAMFREQ.

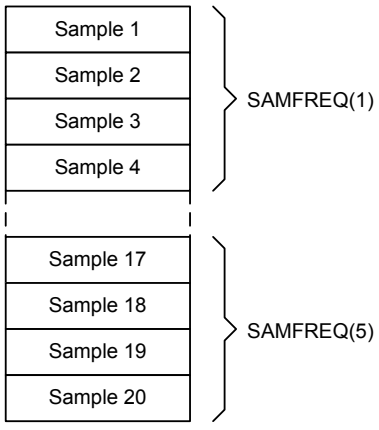

Fig. 18. Cosine filter waveform data window during frequency tracking

In view of the previous analysis, we devise a new timing scheme (patent pending) represented in Fig. 19. With this new timing scheme, we change the sampling frequency

SAMFREQ only at every 3 cycles or 12 quarters of a cycle. Following a change of the sampling frequency, we define a stabilization interval equal to 1.5 cycles or 6 quarters of a cycle during which no calculation of the angle Ψ_m or the frequency deviation Δf is performed. At the end of the stabilization period, we define an interval of frequency measurement equal to 6 quarters of a cycle. During this interval of frequency measurement, we resume the calculation of Ψ_m, Δf, SIGFREQ, and MESFREQ and we then perform six consecutive frequency measurements.

Following a change in the sampling frequency, the stabilization period removes any transient in the phasor calculation resulting from the change in the sampling frequency. We are using a Cosine-type filtering system with a response time of one and a quarter cycles, so we set the stabilization period to one and a half cycles. Following the stabilization period, all the subsequent phasor calculations will be performed with instantaneous values of the waveforms sampled at the same sampling frequency.

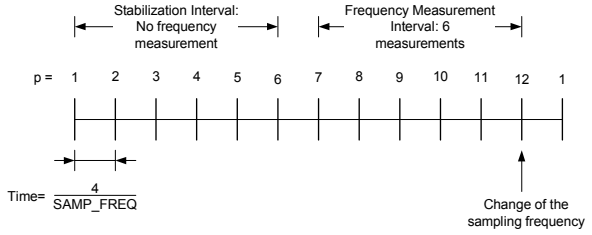

Fig. 19. Second timing scheme

If we apply the timing scheme of Fig. 19 with P = 6 and M = 6, and we inject in the relay a frequency step of 61.75 Hz, we obtain the time trajectory for MESFREQ of Fig. 20. We can see that we obtain the ideal response of Fig. 12. The response time is three cycles, and we have zero overshoot. Progression to the step-frequency value is linear. We have achieved our goal of an ideal response to a step-function.

Fig. 21 represents the corresponding time trajectory of the sampling frequency SAMFREQ. A close examination of the variation of MESFREQ and SAMFREQ indicates that the two variables have become now completely independent. When we apply the 61.75 Hz-step, it takes three cycles with a sampling frequency of 960 Hz to get to the proper frequency measurement MESFREQ of 61.75 Hz. Subsequently, when SAMFREQ slowly increases every three cycles, MESFREQ is not affected by these variations and remains at 61.75 Hz irrespective of the value of SAMFREQ.

We can verify the same properties on Fig. 22, which represents the response to a frequency-step of 57 Hz. Here we have combined the trajectory of MESFREQ together with the time-trajectory of SAMFREQ divided by 16. Again, one can see that the measurement MESFREQ is independent from the sampling frequency SAMFREQ.

When applying frequency steps on the relay, the absolute error in the frequency measurement was found to be better than ±0.005 Hz after the delay of three cycles elapsed.

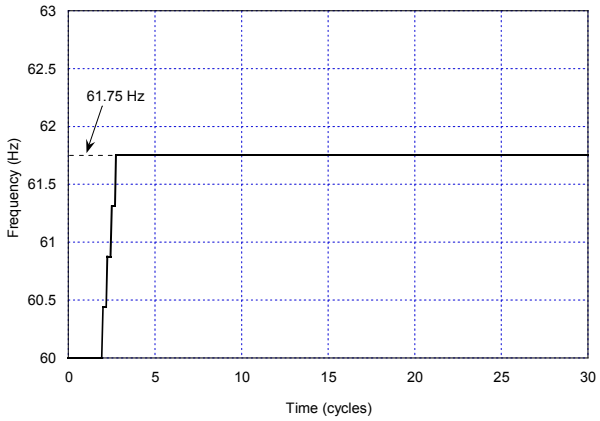

Fig. 20. Frequency measurement time response to a 61.75 Hz step (MESFREQ averaged over 1.5 cycles or M=6)

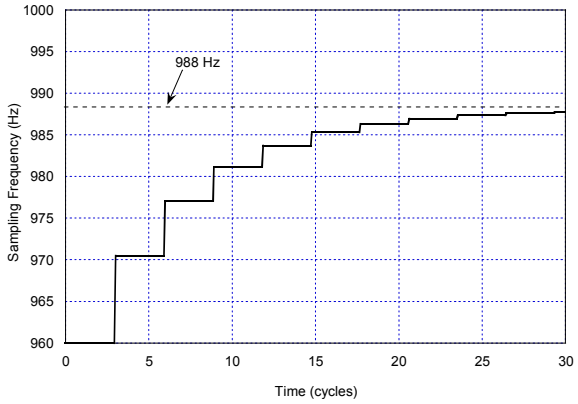

Fig. 21. Sampling frequency time response to a 61.75 Hz step

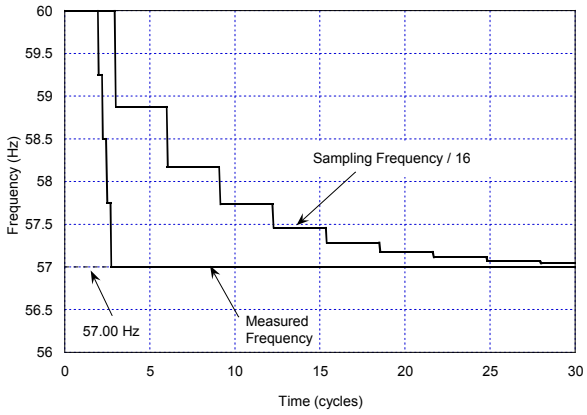

Fig. 22. MESFREQ and SAMFREQ time responses to a 57.00 Hz step

VI. Frequency Measurement Performance Testing

The frequency-step tests we just discussed have been convenient for evaluating the dynamics of the frequency measurement in conjunction with the one for the phase-locked loop that establishes the sampling frequency. On a real network, there are two types of frequency excursions that will occur and that could help to further evaluate the quality of the frequency measurement: frequency ramping and power swing.

Frequency ramping occurs when there is an unbalance between generated power and load on a network. Positive ramping will occur when there is more generation than load

whereas negative ramping will take place when there is more load than generated power.

Fig. 23 represents the frequency measurement with a signal ramping frequency of –0.5 Hz/s. The same plot represents the reference frequency and the sampling frequency. We can see that the delay in the frequency measurement never exceeds three cycles. Also noticeable is the delay between the establishment of the sampling frequency and the measured frequency.

In Section II, we presented an example of a mho element misoperation resulting from a frequency excursion consisting of a ramp of –0.5 Hz/s. If for the same waveforms, the sampling frequency of Fig. 23 is applied, we obtain for the angle between the operating and the polarizing vectors shown in Fig. 24. One can see now that the angle never gets below 90 degrees and the mho element remains stable. Fig. 25 shows the impact of the frequency tracking on the mho element and one can see that the scalar product, as expected, never crosses the line zero. Finally, in Fig. 26, we can see the impact of the frequency tracking on the A-phase voltage. The slight mismatch between the signal and the sampling frequencies is such that the error in the phasor calculation never exceeds 0.5 percent.

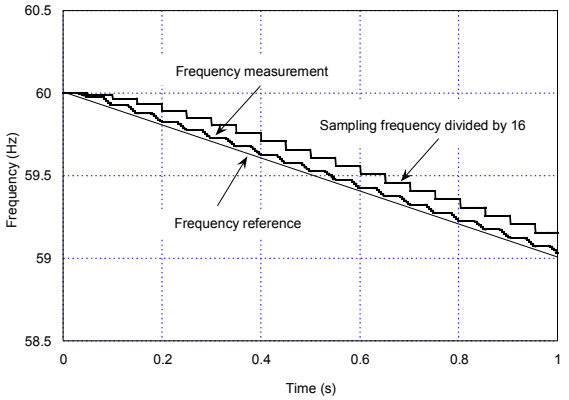

Fig. 23. Frequency measurement and sampling frequency with a ramp of slope equal to –0.5 Hz/s

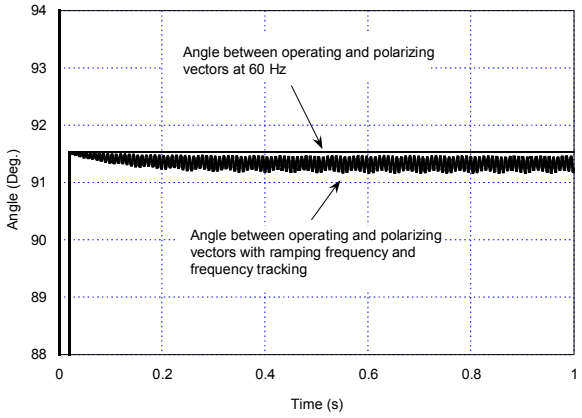

Fig. 24. Angle between operating and polarizing vectors at 60 Hz and with ramping accompanied by frequency tracking

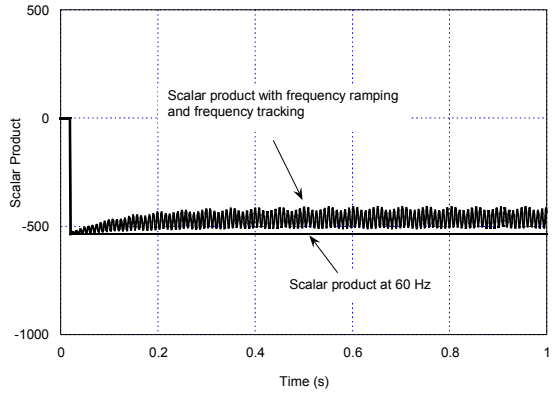

Fig. 25. Scalar product of mho AB element with ramping frequency and frequency tracking

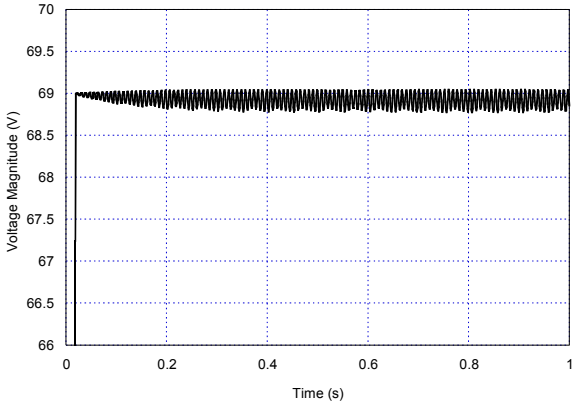

Fig. 26. Magnitude of VA voltage phasor with frequency tracking

Power swings will develop on a network following a major disturbance like a short-circuit, the loss of a major load center, or a generator rejection. We can simulate power-swing-like waveforms by modulating the phase angle of a power source as shown in Annex I. As described in the Annex, we will use a sinewave to modulate the phase angle of one of the two sources of an elementary network. With the parameters selected as V = 100 V, k = 2 and $\omega = 2\pi$ rad/s (corresponding to 1 Hz), we obtain an A-phase waveform the phasor of which has the following time-varying magnitude at the swing-center voltage:

$$\left|\overline{V_{SCV}}\right| = 50 \bullet \sqrt{2[1+\cos(2 \bullet \cos(2\pi t))]} \qquad (27)$$

The phase A voltage phasor at the SCV has a time-varying phase angle equal to the following:

$$\angle\overline{V_{SCV}} = \cos(2\pi t) \qquad (28)$$

The signal frequency in Hertz of the SCV waveform is equal to the derivative of the instantaneous phase:

$$\text{frequency (Hertz)} = 60 - \sin(2\pi t) \qquad (29)$$

When we apply the three-phase voltages to the relay with the frequency tracking operational, we obtain the frequency measurement shown in Fig. 27. The reference frequency corresponds simply to (29). Fig. 28 represents the trajectory of the sampling frequency divided by 16 together with the measured frequency. Finally, Fig. 29 represents the A-phase

time-voltage waveform together with the magnitude the Cosine filtering system acquired for this waveform.

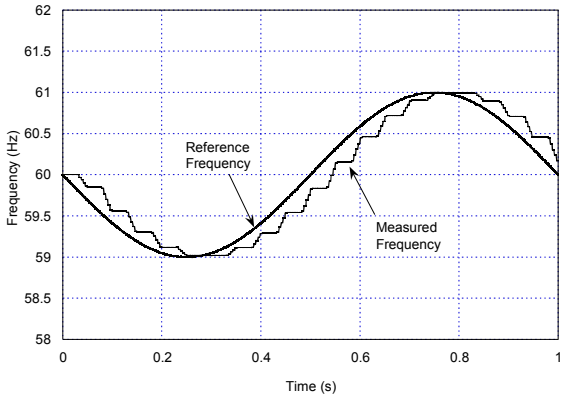

Fig. 27. Power swing frequency measurement

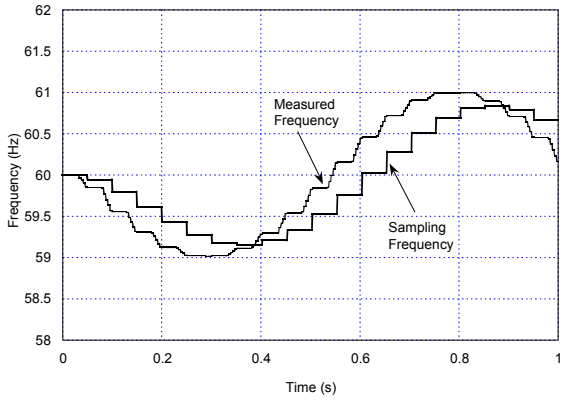

Fig. 28. Power swing frequency and sampling frequency

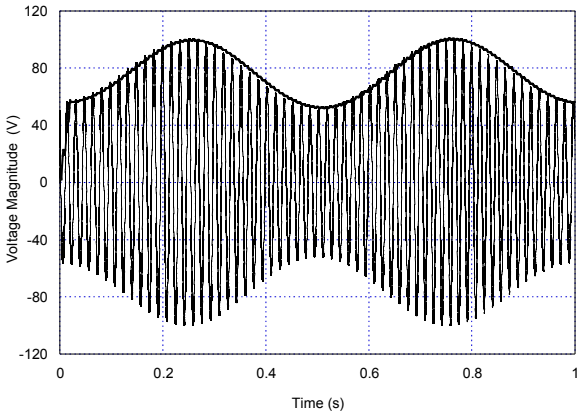

Fig. 29. A-phase voltage during power swing test

VII. Practical Implementation of 81 Elements in a Digital Relay

Once the filtered measurement of the frequency MESFREQ is available, and provided the frequency measurement complies with the basic requirements this paper already expressed, the implementation of 81 frequency elements is relatively simple. We review this implementation here for the sake of completeness.

An overfrequency (81O) or underfrequency (81U) element is simply implemented by comparing the filtered frequency measurement to a threshold and then following the resulting Boolean variable with an adjustable definite time delay.

Fig. 30 shows the logic of a frequency element that can serve either as an 81O or an 81U function. We have the following nomenclature:

FNOM = rated frequency (60 or 50 Hz)

MESFREQ = filtered frequency measurement

81XnTP = frequency pickup value

FREQTROK = frequency tracking okay signal (Boolean)

81XnTD = timer pickup value delay

81XnT = 81 element status (Boolean)

The logic represents an overfrequency element if the pickup threshold is greater than the rated frequency FNOM. Alternatively, it represents an underfrequency element if the pickup threshold is smaller than the rated frequency FNOM. If set as an overfrequency function, the element will assert if the measured frequency is greater than the threshold 81XnTP and after the delay 81XnTD has elapsed. If set as an underfrequency function, the element will assert if the measured frequency is smaller than the threshold 81XnTP and after the delay 81XnTD has elapsed.

Typically, a relay will have at least six elements of this type.

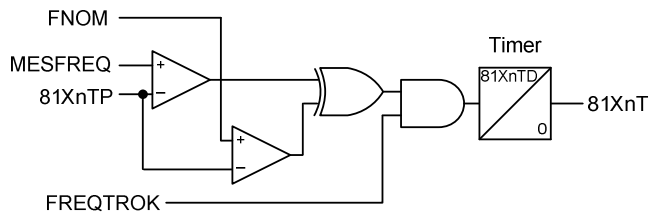

Fig. 30. 81 element logic

VIII. Conclusion

1. Many relays accomplish frequency measurement directly on the voltage input waveforms before waveforms are sampled. For these relays, frequency measurement and frequency tracking are intrinsically independent.
2. For relays that use an adaptive principle to accomplish frequency measurement after sampling voltage and current waveforms, it is necessary to apply at least two basic rules in order to make the frequency measurement independent from the sampling frequency.
   a. No frequency measurement should be made following a change to the sampling frequency during an interval of time equal or greater than the response time of the filtering system using for the computation of the phasors.
   b. No sampling frequency change should be performed before the complete filtering interval required by the frequency measurement filtering is terminated.

3. The time-response trajectory to a frequency-step is a powerful test to determine the dynamics of the frequency measurement.
4. For the purpose of implementing 81 elements in a relay, we want a time response of two to five cycles with a minimum (ideally zero) overshoot.
5. The use of 81 elements requires a steady-state minimum absolute accuracy of 0.01 Hz. Some digital relays achieve accuracy better than 0.005 Hz.
6. Step-response and steady-state accuracy tests should be supplemented with response to frequency ramping functions and power-swing waveforms as defined in the paper.

IX. Appendix: Derivation of Power Swing-Like Waveforms

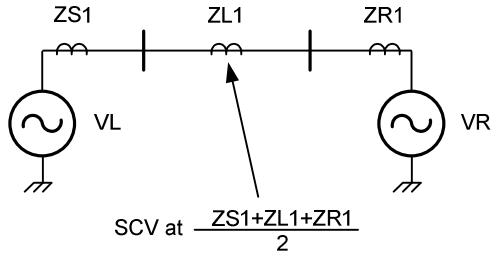

Fig. 31. Elementary network for power swing simulation

Consider the elementary network represented in Fig. 31 and assume that the right-side voltage sources are fixed and provided as follows:

$$\begin{aligned} VRA &= V \bullet \cos(\omega_0 t) \\ VRB &= V \bullet \cos(\omega_0 t - 120°) \\ VRC &= V \bullet \cos(\omega_0 t + 120°) \end{aligned} \tag{30}$$

In (30), ω_0 is the rated frequency. A sinewave modulates the phase for the left-side voltage sources so that we have the following:

$$\begin{aligned} VLA &= V \bullet \cos[\omega_0 t + k \bullet \cos(\omega t)] \\ VLB &= V \bullet \cos[\omega_0 t + k \bullet \cos(\omega t) - 120°] \\ VLC &= V \bullet \cos[\omega_0 t + k \bullet \cos(\omega t)] + 120° \end{aligned} \tag{31}$$

In this last equation, ω is the phase angle modulation frequency. The following equation provides A-phase voltage at the swing center voltage (SCV):

$$V_{SCV} = \frac{VLA + VRA}{2} \tag{32}$$

We then have the following:

$$V_{SCV} = \frac{V}{2} \bullet \{\cos[\omega_0 t + k \bullet \cos(\omega t)] + \cos(\omega_0 t)\} \tag{33}$$

After a few manipulations, we express V_{SCV} as:

$$V_{SCV} = \frac{V}{2} \bullet \sqrt{2[1 + \cos(k \bullet \cos(\omega t))]} \bullet \left\{\cos(\omega_0 t + \frac{k \bullet \cos(\omega t)}{2})\right\} \tag{34}$$

The V_{SCV} phasor has a time-varying magnitude equal to:

$$\left|\overline{V_{SCV}}\right| = \frac{V}{2} \bullet \sqrt{2[1 + \cos(k \bullet \cos(\omega t))]} \tag{35}$$

The V_{SCV} phasor has a time-varying phase angle equal to:

$$\angle\overline{V_{SCV}} = \frac{k \bullet \cos(\omega t)}{2} \tag{36}$$

The frequency of the SCV waveform is equal to the derivative of the instantaneous phase:

$$\begin{aligned} \text{frequency} &= \frac{d}{dt}\left(w_0 t + \frac{k \bullet \cos(\omega t)}{2}\right) \\ &= \omega_0 - \frac{k \bullet \omega \bullet \sin(\omega t)}{2} \end{aligned} \tag{37}$$

In units of Hertz, the frequency is given as:

$$\text{frequency (Hertz)} = \frac{2\omega_0 - k \bullet \omega \bullet \sin(\omega t)}{4\pi} \tag{38}$$

X. References

[1] Tou, Julius T., *Modern Control Theory*. New York: McGraw-Hill, 1964.

[2] Shinners, Stanley M., *Modern Control System Theory and Design*. New York: J. Wiley Interscience, 1992.

[3] E. O. Schweitzer, III and D. Hou, "Filtering for Protective Relays," 19th Annual Western Protective Relay Conference, Spokane, WA, October 1992.

[4] E. O. Schweitzer, III and J. Roberts, "Distance Relay Element Design," 19th Annual Western Protective Relay Conference, Spokane, WA, October 1992.

[5] R. Cimadevilla, R. Quintanilla, S. Ward, "Adapting Protection to Frequency Changes," 32nd Annual Western Protective Relay Conference, Spokane, WA, October 25-27, 2005.

[6] B. Kasztenny, D. Finney, I. Voloh, "Impact of Frequency Deviations on Protective Functions," 34th Annual Western Protective Relay Conference, Spokane, WA, October 16-18, 2007.

[7] D. Hou, "Relay Element Performance During Power System Frequency Excursions," 34th Annual Western Protective Relay Conference, Spokane, WA, October 16-18, 2007.

[8] A.G. Phadke, J.S. Thorpe, M.G Adamiak, "A New Measurement Technique for Tracking Volatge Phasors, Local System Frequency and Rate of Change of Frequency," IEEE Trans., Vol. PAS-102, No. 5, pp. 1025-1038, 1983.

[9] G. Benmouyal, "An Adaptive Sampling Interval Generator for Digital Relaying," *IEEE Transactions on Power Delivery*, Vol. 4, No. 3, pp. 1602-9, July 1989.

[10] G. Benmouyal, "Removal of DC-Offset in Current Waveform Using Digital Mimic Filtering," *IEEE Transactions on Power Delivery*, Vol. 10, No. 2, p. 621-630, April 1995.

[11] William Premerlani, "Digital Phase-Locked Loop and Frequency Measuring Device," U.S. Patent 4, 715, 000, Dec. 22, 1987.

[12] Armando Guzman-Casillas, Gabriel Benmouyal, "System for Estimating the Frequency of the Power Signal on a Power Transmission Line," US Patent .6, 603, 298, Aug. 5, 2003.

XI. Biographies

Gabriel Benmouyal, P.E. received his B.A.Sc. in Electrical Engineering and his M.A.Sc. in Control Engineering from Ecole Polytechnique, Université de Montréal, Canada in 1968 and 1970, respectively. In 1969, he joined Hydro-Québec as an Instrumentation and Control Specialist. He worked on different projects in the field of substation control systems and dispatching centers. In 1978, he joined IREQ, where his main field of activity has been the application of microprocessors and digital techniques for substation and generating-station control and protection systems. In 1997, he joined Schweitzer Engineering Laboratories in the position of Principal Research Engineer. He is a registered professional engineer in the Province of Québec, is an IEEE Senior Member, and has served on the Power System Relaying Committee since May 1989. He holds over six patents and is the author or co-author of several papers in the field of signal processing and power networks protection and control.

Angelo D'Aversa received from Drexel University his BSEE degree in 1990 and an MSEE degree in 1994. After graduation he developed distribution relays for General Electric for 9 years. In 1999 he joined Schweitzer Engineering Laboratories as a test engineer and since joining SEL has spent many years developing firmware for a variety of protective relays. Presently, he is R&D Manager for the Industrial Systems group for SEL. Industrial Systems specializes in motor and generator relays for Industrials and Utilities.